

Is there a specific magnetic resonance phenotype characteristic of hereditary breast cancer?

Giovanna Trecate¹, Siranuosh Manoukian², Laura Suman³, Daniele Vergnaghi¹, Monica Marchesini³, Roberto Agresti⁴, Cristina Ferraris⁴, Bernard Peissel², Davide Scaramuzza¹, and Silvana Bergonzi³

¹Unit of Diagnostic Radiology "1", ²Department of Experimental Oncology-Medical Genetics, ³Unit of Diagnostic Radiology "3", and ⁴Unit of Breast Surgery, Fondazione IRCCS Istituto Nazionale dei Tumori, Milan, Italy

ABSTRACT

Aims and background. The aim of the study was to investigate the growth rate of inherited breast cancer, to analyze its T2 signal intensity besides kinetic and morphologic aspects, and to verify whether there is any correlation between magnetic resonance imaging phenotype and BRCA status.

Methods. Between June 2000 and September 2009, we enrolled 227 women at high genetic risk for breast cancer in a surveillance program, within a multicenter project of the *Istituto Superiore di Sanità* (Rome).

Results. Thirty-four cancers were detected among 31 subjects. One patient refused magnetic resonance imaging because of claustrophobia. Compared with sporadic disease, hereditary cancer showed some differences, in terms of biologic attitude and semeiotic patterns. These differences were mainly registered for magnetic resonance imaging, where the most frequent radiological variant was represented by the very high T2 signal intensity (73%). Moreover, the size of 8 of the neoplasms showed a significant increase in less than one year, 5 of them in less than 6 months. Six lesions were in BRCA1 patients and the remaining in BRCA2. Furthermore, cancers with a high growth rate also demonstrated a significant increment in T2 signal intensity.

Conclusions. Our results confirmed the high growth rate within BRCA-related breast cancers, especially for BRCA1 mutation carriers. In our experience, we found a specific imaging phenotype, represented by the high T2 signal intensity of hereditary breast cancer. To our knowledge, this is the first report that points out this new semeiotic parameter, which is usually typical of benign lesions. Considering the correlation between high growth rate and high T2 signal intensity, the former seems to be related to the absence of induction of a desmoplastic reaction that could somehow restrict cancer growth. Free full text available at www.tumorionline.it

Introduction

In the 1990s the concept of inherited breast cancer was focused on. In fact, two breast-related cancer genes, BRCA1 and BRCA2, were identified. Mutations in these genes are responsible for a markedly increased risk to develop breast cancer, even at a young age, which is often multiple. Women BRCA carriers face almost a 60% life-long risk of breast cancer.

The optimal management of this increased risk is still under intense investigation, which includes screening, risk-reducing surgery and chemoprevention^{1,2}. Surveillance has been traditionally based on regular clinical examination and mammography, which currently represents the most effective screening method in the general population. Nevertheless, first reports on the aptitude of mammography in the detection of breast cancer in high-risk women showed a huge percentage of false-negative results³⁻⁵.

Key words: breast cancer, BRCA mutation, growth rate, magnetic resonance imaging, T2 signal intensity.

Acknowledgments: We especially thank Dr.ssa Franca Podo for her competence and devotion to the study of inherited breast cancer.

Correspondence to: Dr Giovanna Trecate, Fondazione IRCCS Istituto Nazionale dei Tumori, via Venezian 1, 20133 Milan, Italy.
Tel +39-02-2390-2547;
fax +39-02-2390-2548;
e-mail
giovanna.trecate@istitutotumori.mi.it

Received February 2, 2010;
accepted February 8, 2010.

Owing to its high spatial and contrast resolution and no X-ray correlation, magnetic resonance imaging (MRI) has been progressively included in screening protocols. The superior sensitivity of the technique for the detection of breast cancer even at an early stage has been unanimously established^{4,6-10}.

At our Institute, between June 2000 and September 2009, 227 women at high genetic risk entered a protocol of diagnostic surveillance: 34 breast cancers were diagnosed in 32 patients. One of them was only diagnosed at mammography and ultrasound because the patient refused MRI examination. During this period, we noticed some differences between the biologic behavior of hereditary cancer compared with sporadic disease.

First of all, we noted that the growth of breast cancer in high-risk patients can be very fast. We registered 8 (23%) cases in which the size of the suspected lesion markedly increased in less than one year, 5 of them in less than 6 months and 2 within 6 months.

Secondly, according to the traditional MRI semeiotic phenotype, we encountered some morphologic or dynamic aspects of the BRCA-related neoplasm that could not be considered as typical for cancer, particularly for the T2 signal intensity (SI), which was very high, as we usually find in benign diseases of the general population. Conventional imaging also registered some differences as regards sporadic cancers.

The aim of the study was to verify the high speed of growth of inherited breast cancer, to study their T2 SI besides kinetic and morphologic aspects, and to analyze whether there was any difference in the MRI phenotype between BRCA1, BRCA2 carriers and women at high familial risk.

Materials and methods

Patients

Between June 2000 and May 2009, 230 women – BRCA1 (136) and BRCA2 carriers (61), or first degree relatives of BRCA1 (4) and BRCA2 (4) carriers, or with high familial risk of breast cancer (25) – were annually screened with clinical examination, mammography, ultrasound and MRI.

Women were classified as BRCA1 or BRCA2 carriers if genetic testing identified a disease-causing mutation. Women belonging to families where no mutation was identified or in whom the test was not performed were classified as high familial risk, according to previously established criteria. Informed consent was obtained from each subject enrolled in the study.

Methods

Mammography was performed in craniocaudal and mediolateral oblique projections. Spot compression,

magnification, and additional views were obtained as needed (Hologic Selenia, direct digital mammography). Ultrasound of the breast was performed with high frequency probes (12-5 MHz, 50 mm) (Philips HDI 5.000).

MRI examinations were performed on a 1.5 T magnet (n. 23 with Magnetom Vision and n. 12 with Magnetom Avanto, Siemens, Erlangen, Germany) using a dedicated double breast surface coil. For premenopausal patients, MRI was performed between the 7th and the 14th day of the menstrual cycle. Our imaging protocol consisted of a previous T2 inversion recovery (IR) sequence (TR/TE 5770/73) followed by a three-dimensional, gradient-echo, T1-weighted dynamic images (TR/TE 7.8/4.7, flip angle 25°, slice thickness 1.8 mm without gap, no. of sections 88, matrix 410 x 512, FOV 340 x 100 cm, TA 55 sec) obtained once before and five times after injection of 0.2 mmol/kg gadolinium DTPA and followed by a saline flush of 20 ml.

Informed consent was obtained before each MRI examination.

Histopathological confirmation was obtained at vacuum-assisted core-needle biopsy with mammography, ultrasound or MRI guidance.

Two dedicated radiologists analyzed mammographic and sonographic aspects of each lesion (Table 1). Another radiologist expert in breast MRI, blinded to the results of conventional analysis, described both morphologic and dynamic aspects of each enhancing region (Table 2). For morphologic characteristics, the analysis was performed on image subtraction of the precontrast images from early and late postcontrast images in order to obtain the suppression of fat and nonenhancing parenchyma and to distinguish the enhancing aspects. Lesion shape (mass like, non-mass like [irregular shape], ductal), dendritic enhancement and margins were evaluated.

For dynamic aspects, a region of interest (ROI) was placed within the tumor-suspected enhancement and the SI-to-time curve was calculated. The shape of the curve (type I, persistent; type II, plateau; type III, washout)¹¹ was also evaluated. Further patterns of MRI analysis were the modality of uptake of contrast medium (homogeneous, heterogeneous, with rim enhancement) and the T2 SI (optically judged as high, intermediate, or low).

For each breast cancer we measured the maximum diameter in case of mass-like enhancement. In case of irregular or dendritic shape enhancement or when multiple small contiguous foci were present, we measured their overall maximum extension, whereas we took the length and the breadth in case of ductal-like enhancement. As the T2 SI did not change when a recall was requested, we quantified T2 SI only on the last MRI examination. When interesting changes in size occurred for the same breast cancer in two different examinations, we measured the two main perpendicular diameters.

Table 1 - Mammographic and ultrasound results

Pt. no.	Age at exam (yr)	Parenchymal pattern	Mass with indistinct margins	Mass with circumscribed margins	Structural distortion	Asymmetric thickening	Suspect calcifications	Benign calcifications	Ill-defined hypoechoic mass	Hypoechoic mass, circumscribed margins	Hypoechoic lobulated mass	Focal architectural distortion	Genetic status	Histology
Mammography														
1	43	N1	+	-	-	-	-	-	+	-11	-	-	BRCA1	IDC
2	60	N1	-	-	-	-	-	-	-	-	-	-	BRCA1	IDC
3	61	N1	-	-	-	+	-	-	-	-	+	-	BRCA1	IDC
4	35	P2	-	-	-	-	-	-	-	-	-	-	BRCA2	ILC+LCIS
5	40	ND	-	-	-	-	-	-	+	-	-	+	HFR	IDC
6	52	N1	ND	ND	ND	ND	ND	ND	ND	-	-	-	BRCA1	IDC
7	48	P2	+	-	-	-	-	-	+	-	-	-	BRCA1	IDC+DCIS
8	63	N1	-	-	-	-	-	-	-	-	-	-	BRCA1	DCIS
9	52	N1	-	-	-	-	+	-	-	-	-	-	BRCA1	IDC
10	38	N1	+	-	-	-	-	-	+	-	-	-	BRCA1	IDC
11	61	P2	-	-	-	-	-	-	-	-	-	-	BRCA2	ND
12	46	P2	+	-	-	-	-	-	+	-	-	-	BRCA1	DCIS
13	56	P1	-	-	-	+	-	-	-	-	-	-	HFR	IDC+DCIS
14	50	DY	-	-	-	-	-	-	-	-	-	-	HFR	DCIS+LCIS
15	41	DY	-	-	-	-	-	-	-	-	-	-	BRCA1	IDC
16	56	P2	-	-	-	-	-	-	-	-	+	-	BRCA1	IDC+DCIS
17	48	N1	-	-	-	-	-	-	-	-	-	+	BRCA2	IDC+ILC
18	59	N1	+	-	-	-	-	-	-	-	-	-	HFR	ITC
19	44	P2	-	-	-	-	-	-	-	-	-	-	BRCA1	IC NAS
20	42	P2	-	-	-	-	-	-	-	-	-	+	BRCA1	IDC+DCIS
21	43	P2	-	-	-	-	-	-	-	-	+	-	BRCA1	IDC+LCIS
22	42	P1	+	-	-	-	-	-	+	-	-	-	BRCA2	IDC+DCIS
23	47	P1	+	-	-	-	-	-	+	-	-	-	BRCA1	IDC
24	54	P2	+	-	-	-	-	-	+	-	-	-	BRCA1	IDC
25	50	N1	-	-	-	-	-	-	-	-	-	-	BRCA2	DCIS+LCIS
26	40	DY	-	-	-	-	-	-	-	-	-	-	BRCA1	IDC
27	63	N1	-	-	-	-	-	-	+	-	+	-	BRCA1	IDC
28	64	P2	-	-	-	-	-	-	+	-	-	-	HFR	IDC+ILC
29	63	DY	-	-	-	-	-	-	+	-	-	-	HFR	IDC
30	52	N1	-	-	-	-	-	-	+	-	-	-	BRCA2	IDC+DCIS
31	52	N1	-	-	-	-	-	-	-	-	-	-	BRCA2	IDC+DCIS

mo, months; rt, right; lt, left; rc, recall. (continued)

(continued) **Table 1**

Pt. no.	Age at exam (yr)	Parenchymal pattern	Mass with indistinct margins	Mass with circumscribed margins	Structural distortion	Asymmetric thickening	Suspect calcifications	Benign calcifications	Ill-defined hypoechoic mass	Hypoechoic mass, circumscribed margins	Hypoechoic lobulated mass	Focal architectural distortion	Genetic status	Histology
31	37	P2	-	-	-	-	-	-	-	-	-	-	BRCA1	IDC+DCIS
32	56	P2	-	-	-	-	-	-	+	-	-	-	BRCA1	LCIS+ductal hyperplasia with atypical foci
33	39	P2	-	-	-	-	-	-	-	-	-	-	BRCA1	Adenosis
34	48	P2	-	-	-	-	-	-	-	-	-	-	BRCA1	Adenosis
35	37	DY	-	-	-	-	+	-	-	-	-	-	BRCA1	Dysplasia
36	40	P2	-	-	-	-	-	-	+	-	-	-	HFR	Dysplasia
37	54	P2	-	-	-	-	-	-	-	-	-	-	BRCA1	Dysplasia
38	45	P2	-	-	-	-	-	-	-	+	-	-	BRCA1	Phyllodes tumor

rc, recall; mo, months.

Case 11: In the right breast, the patient had 1 lesion; in the left, a major lesion (A) and a smaller lesion (B).

Table 2 - MRI morphologic-kinetic phenotype

Pt no.	Age (yr)	Morphologic shape	Margins	Internal enhancement	Location	Dynamic curve	T2 SI	Histology	Genetic status
1	43	Oval mass-like enhancement	Irregular	Homogeneous	Central quadrant prepectoral	Washout	Very high	IDC	BRCA1
2	60	Round mass-like enhancement	Smooth	Homogeneous	Central quadrant	Plateau	Very high	IDC	BRCA1
3	61	Round mass-like enhancement	Smooth	Homogeneous	Lower outer	Plateau	Not done	IDC	BRCA1
4	35	Round mass-like enhancement (2 contiguous)	Irregular	Rim enhancement	Left-upper inner prepectoral	Washout	Very high	ILC + LCIS	BRCA2
5	40	Round mass-like enhancement	Irregular	Rim enhancement	Right-upper inner nipple infiltration	Washout	Very high	IDC	
6	58	Round mass-like enhancement	Irregular	Homogeneous	Lower outer	Washout	ND	IDC	HFR
7	52	Round mass-like enhancement (some small contiguous)	Irregular	Homogeneous	Upper inner	Washout	Very high	IDC	BRCA1
8	rc 5 mo	Unchanged	Irregular	Homogeneous	Central quadrant	Washout	Very high	IDC + DCIS	BRCA1
9	48	Round mass-like enhancement	Smooth	Homogeneous	Upper outer prepectoral	Washout	Very high	IDC + DCIS	BRCA1
10	63	Dendritic enhancement (10x2 mm)	Irregular	Heterogeneous	Central quadrant	Steady	Intermediate	DCIS	
11	rc 3 mo	Oval mass like enhancement (one single 15 mm)	Irregular	Homogeneous	Upper outer prepectoral	Steady	Intermediate		
12	52	Oval mass-like enhancement	Smooth	Homogeneous	Central quadrant	Washout	Very high	IDC	BRCA1
13	38	Oval mass-like enhancement (2 contiguous)	Irregular	Homogeneous	Upper inner	Washout	Low	IDC	BRCA1
14	61 rt	Irregular shape (not mass like)	Irregular	Homogeneous	Right-upper outer prepectoral	Plateau	Low	ND	BRCA2
15	61 l a)	Round mass-like enhancement	Irregular	Rim enhancement	Left-lower outer	Washout	Very high	IDC	
16	61 l b)	Irregular shape (not mass like)	Irregular	Homogeneous	Left-upper outer prepectoral	Washout	Very high	DCIS	
17	46	Round mass-like enhancement (many contiguous)	Irregular	Homogeneous	Upper inner	Steady	Intermediate	IDC	BRCA1
18	56	Not done	-	-	-	-	-	IDC + DCIS	HFR
19	50	Irregular shape (not mass like)	Irregular	Heterogeneous	Central quadrant	Washout with delay as lobular type	Intermediate	DCIS + LCIS	HFR
20	rc 7 mo	Unchanged	Irregular	Homogeneous	Upper inner prepectoral	Unchanged			
21	41	Round mass-like enhancement (2 small contiguous)	Smooth	Homogeneous	Central quadrant	Plateau	Very high	IDC + DCIS	BRCA1
22	56	Round mass-like small contiguous foci (5 x 18 mm)	Smooth	Homogeneous	Upper inner prepectoral	Wash out	Very high	IDC + DCIS	BRCA1
23	rc 3 mo	Irregular shape (non mass like) with several contiguous dendritic aspects (18 x 10 mm)	Irregular	Homogeneous	Central quadrant	Wash out	Very high		
24	48	Ductal enhancement (8 x 2 mm)	Irregular	Homogeneous	Central quadrant	Wash out	Low	IDC + ILC	BRCA2
25	rc 6 mo	Round mass like enhancement (some contiguous) 10 x 4 mm	Irregular	Homogeneous	Upper outer	Wash out	Low		
26	59	Round mass like enhancement	Irregular	Homogeneous	Upper outer	Wash out	ND	Invasive tubular carcinoma	HFR

rc, recall; mo, months.

(continued)

(continued) **Table 2**

Pt no.	Age (yr)	Morphologic shape	Margins	Internal enhancement	Location	Dynamic curve	T2 SI	Histology	Genetic status
19	44	Round mass like enhancement (6 mm)	Smooth	Homogeneous	Upper outer posterior portion of the breast	Steady	Very high	Invasive carcinoma	BRCA1
	rc 4 mo	Oval mass like enhancement (14 mm)	Irregular	Rim enhancement		Steady	Very high		
20	42	Round mass like enhancement	Smooth	Homogeneous	Upper outer prepectoral	Wash out	Middle	IDC + DCIS	BRCA1
21	43	Oval mass like enhancement	Irregular	Rim enhancement	Upper outer prepectoral	Steady	Middle	IDC + LCIS	BRCA1
22	42	Round mass like enhancement	Irregular	Rim enhancement	Upper inner posterior portion of the breast	Plateau	Very high	IDC + DCIS	BRCA2
23	47	Round mass like enhancement (1 x 13 mm)	Irregular	Homogeneous	Central quadrant prepectoral	Wash out	Very high		BRCA1
	rc 3 mo	Round mass like enhancement (15 x 20 mm associated to two more)	Irregular	Homogeneous	Prepectoral	Steady	Very high		
		Round mass like enhancement (7 and 6 mm)	Irregular	Homogeneous	Prepectoral	Steady	Very high	IDC	
24	54	Dendritic Enhancement (5 x 18 mm)	Irregular	Heterogeneous	Central quadrant	Plateau	Very high		BRCA1
	rc 12 mo	Round mass like enhancement (12 x 18 mm)	Irregular	Rim enhancement	Central quadrant	Plateau	Very high	IDC	
25	50	Oval mass like enhancement (some small contiguous)	Smooth	Homogeneous	Upper outer	Wash out	Very high		BRCA2
	rc 4 mo	Unchanged	Smooth	Homogeneous	Upper outer	Wash out	Very high	DCIS + LCIS	
26	40	Round mass like enhancement	Irregular	Rim enhancement	Upper outer prepectoral	Wash out	Very high	IDC	BRCA1
27	63	Round mass like enhancement	Smooth	Homogeneous	Central quadrant	Plateau	Very high	IDC	BRCA1
28	64	Round mass like enhancement (some contiguous within scar)	Irregular	Heterogeneous	Lower outer prepectoral	Wash out	Very high	IDC + ILC	HFR
29	63	Irregular Shape (Non mass like)	Irregular	Homogeneous	Upper outer prepectoral	Wash out and steady	Very high	IDC	HFR
	rc 4 mo	Unchanged	Irregular	Homogeneous	Upper outer prepectoral	Wash out only	Very high		
30	52	Round mass like enhancement (8 mm)	Smooth	Homogeneous	Upper outer	Wash out only	Very high		
	rc 6 mo	Round mass like enhancement + IrregularFlare (12mm)	Irregular	Homogeneous	Upper outer	Wash out	Very high	IDC + DCIS	BRCA2
31	37	Round mass like enhancement (some contiguous) 16mm	Irregular	Homogeneous	Upper inner	Wash out	Very high	IDC+DCIS	BRCA1
	rc 4 mo	Round mass like enhancement (many contiguous) 33mm	Irregular	Homogeneous	Upper inner	Wash out	Very high		
32	56	Round mass like enhancement	Smooth	Homogeneous	Lower outer	Wash out	Very high	LCIS + ductal	BRCA1
								iperplasia with atypical foci	
33	39	Irregular shape (Non mass like)	Irregular	Heterogeneous	Upper inner	Steady	Isointensity	Adenosis	BRCA1
34	48	Oval mass like enhancement	Smooth	Homogeneous	Upper inner	Plateau	Very high	Adenosis	BRCA1
35	37	Irregular shape (Non mass like)	Irregular	Homogeneous	Upper inner	Plateau	Intermediate	Dysplasia	BRCA1
36	40	No suspected results						Benign disease	HFR
37	54	No suspected results						Stromal fibrosis	BRCA1
38	45	Round mass like enhancement	Smooth	Homogeneous	Sovra-areolar	Aspecific	Very high	Phyllodes tumor	BRCA1

IDC, invasive ductal carcinoma; DCIS, ductal carcinoma *in situ*; ILC, invasive lobular carcinoma; LCIS, lobular carcinoma *in situ*; HFR, high familial risk; rc, recall; ND, not done; mo, months.

The radiographic tumor size ranged from 4 mm to 3 cm.

To quantify the optical brightness of T2 SI, we first applied the “pixel lens value” function (Table 3). On the T2-weighted IR fat-suppressed sequence, we scheduled a mean SI value of each lesion by computing 3 measurements and deriving the mean SI mean. Despite the well-known overall nonhomogeneity of breast parenchyma, we tried to relate the SI of the lesion to that of the mammary gland. In order to accomplish this, we choose to draw 3 pixel lens values within the normal tissue surrounding the lesion, irrespective of its content, then derived the mean value. We kept a distance of 10 mm as regards the lesion to avoid any overlap with eventual neoangiogenetic vessels or desmoplastic reactions. The mean results were compared to calculate the ratio between the T2 SI of the lesion and that of the surrounding breast (LPS, lesion-to-parenchyma signal score).

On T2-weighted IR fat-suppressed sequences, we also calculated a mean SI value by means of an ROI (Table 3). For this second procedure, we applied the evaluation on the pectoralis major muscle in the region of its major thickness and on the suspected neoplastic lesion. Since the lesion size of our cohort ranged from 5 mm to 3 cm, we selected two different ROIs with a mean diameter of 5.0 ± 0.1 mm for each lesion, then averaged the SI results. Only for one lesion no larger than 2 mm was the ROI diameter small enough to fit the right size of the lesion in analysis. Final values were calculated by dividing the lesion SI by the SI of the major pectoral muscle (LMS, lesion-to-muscle signal score).

In order to yield uniform results, we held the same ROI diameter for analysis of the T2 SI of the pectoralis major muscle. In this second case, the mean results were also compared and final values were calculated by dividing the T2 SI value of the lesion by that of the pectoralis major muscle.

Once all the ratio scores were calculated, we determined some threshold values to quantify optical impressions. When a suspected finding was seen at only MRI despite ultrasound second look, recall of the patient was recommended. The recall was mainly advised because of the very small diameter of the lesions at their presentation, because of the occurrence of benign morphologic-kinetic features for some cases, and because of the unavailability of the MRI-guided biopsy device until April 2009.

Results

Between June 2000 and May 2009, 227 women at high genetic risk were enrolled in the study. During this period, 34 breast cancers were diagnosed in 31 women. Nineteen breast cancers were detected in 19 BRCA1 carriers (19/34, 61%), 9 in 6 BRCA2 carriers (9/34, 29%), and 6 in 6 women at high familial risk (6/34, 19%). Patient 5 and patient 11 were submitted to conventional analysis

at another hospital and directed to MRI in our Institution (patient 11 had two enhancing lesions in the left and one in the right breast). For another woman, cancer was diagnosed only by means of conventional imaging as the patient refused MRI because of claustrophobia (patient 13). The 34th neoplasm was detected in a carrier who had a contralateral breast cancer 5 years after mastectomy. Of the 34 diagnosed breast cancers of our cohort, only 33 were evaluated by means of MRI because 1 patient refused the examination.

All of the 33 breast cancers submitted to MRI analysis were detected by this modality. For one of these patients, conventional imaging was not available but was reported as negative. Nine cancers were detected also with mammography, and 3 cancers became suspect at the recall (12/34, 35.2%). Eighteen cancers were detected also with ultrasound and 4 become recognizable at the recall (22/34, 64.7%). Nine women had already developed cancer in the contralateral breast before enrollment, and 4 had an ipsilateral breast cancer.

MRI registered 3 false-positive results (patients 33, 34, 35); 2 were found to be adenosis, and 1 was a complex dysplasia at histological examination. Conventional imaging registered 3 false-positive reports, not confirmed at MRI and histology (patients 36, 37 and 38).

In one case, MRI and ultrasound disclosed a focus of lobular carcinoma *in situ* (LCIS) (patient 32). According to the international guidelines, this case was not considered as a true carcinoma.

Histology

Table 4 summarizes the histological features of the 34 detected breast cancers. Of these, 18 were pure invasive cancers, 2 were pure ductal carcinoma *in situ* (DCIS), 1 was a DCIS and LCIS, and 11 were invasive carcinomas with *in situ* components. Histological type was not available in one patient for whom invasive carcinoma not otherwise specified was reported (patient 19). Moreover, patient 11 had bilateral pathological features at imaging; she was treated after our diagnosis at another institution, where following left lesion biopsy she received chemotherapy; subsequent MRI evaluation showed good regression of the disease in both breasts. The patient underwent left mastectomy and continued her further follow-up at the other institution.

Within the invasive group, the most common histological type was ductal carcinoma (IDC), described in 25/34 cases (73%). IDC was present in 17 of the 19 cancers in BRCA1 carriers, in 5 of 8 cancers in BRCA2 carriers, and in 3 of 6 cancers in high-familial-risk patients. IDC were mostly grade III (20/34, 59%), and only 2 cases were grade I (one in the tubular carcinoma and one in an IDC of a BRCA2 carrier).

Although receptor and Her2-neu status was not available for all cases, we found 9 triple negatives, 8 of which were in tumors of BRCA1 carriers.

Table 3 - T2 signal intensity quantification

Pt no.	Age at exam	Genetic status	Histology	Grade	T2 SI Muscle/parenchyma score LMS	T2 SI Lesion/parenchyma score LPS	Lesion size	MR Device
1	43	BRCA1	IDC with medullary aspects	III	O = very high L = 350 M = 91 LMS = 3.8	O = very high L = 500 P = 130 LPS = 3.8	12 mm mass-like enh.	Vision
2	60	BRCA1	IDC	III	O = very high L = 234.5 M = 35 LMS = 6.7	O = very high L = 300 P = 50 LPS = 6	5 mm mass-like enh.	Avanto
3	61	BRCA1	IDC	ND	ND	ND	6 mm mass-like enh.	Vision
4	35	BRCA2	ILC + LCIS	III	O = very high L = 541 M = 127 LMS = 4.2	O = very high L = 560 P = 200 LPS = 2.8	5 + 12 mm mass-like enh.	Vision
	40		IDC	II	O = very high L = 367 M = 38 LMS = 9.6	O = very high L = 382 P = 100 LPS = 3.8	13 mm mass-like enh.1	Avanto
5	58	HFR	IDC	I	ND	ND	10 mm mass-like enh.	Vision
6	52	BRCA1	IDC	III	O = very high L = 591 M = 115 LMS = 5.1	O = very high L = 700 P = 160 LPS = 4.3	8 mm mass-like enh. rc 5 mo, 8 mm mass-like enh.	Vision
7	48	BRCA1	IDC with medullary aspects + DCIS	III	O = very high L = 410 M = 89.5 LMS = 4.5	O = very high L = 390 P = 130 LPS = 3	7 mm mass-like enh.	Vision
8	63	BRCA1	DCIS	III	O = intermediate intensity L = 92 M = 61 LMS = 1.5	O = intermediate intensity L = 108 P = 52 LPS = 2	10 x 2 mm ductal-like enh. rc 3 mo, 15 x 3 mm mass-like enh.	Avanto
9	52	BRCA1	IDC	II	O = very high L = 551 M = 126.5 LMS = 4.3	O = very high L = 500 P = 120 LPS = 4	8 mm mass-like enh.	Vision
10	38	BRCA1	IDC	III	O = low intensity L = 650.5 M = 110.5 LMS = 5.9	O = low intensity L = 650 P = 960 LPS = 0.67	5 + 7 mm mass-like enh.	Vision
11	61	BRCA2	right no biopsy	III	Right O-low intensity L = 233 M=93 LMS = 2.5	Right O-low intensity L = 200 P = 160 LPS = 1.2	right 15 mm irregular shape	Vision
			left a) IDC		O = very high L = 690.5 M = 93 LMS = 7.4	O = very high L = 550 P = 160 LPS = 3.4	left a) 25 mm mass-like enh. + 15 mm irregular shape	
			left b) DCIS		O = very high L = 385 M = 93 LMS = 4.1	O = very high L = 790 P = 160 LPS = 4.9	left b) 10 mm irregular shape	
12	46	BRCA1	IDC	III	O = intermediate intensity L = 466.5 M = 119.5 LMS = 3.9	O = intermediate intensity L = 300 P = 170 LPS = 1.7	20 mm mass-like enh.	Vision
13	56	HFR	IDC pure mucinous subtype + DCIS	III	ND	ND		ND
14	50	HFR	DCIS + LCIS + pagetic extension to ducts	II	O = intermediate intensity L = 508 M = 139.5 LMS = 3.6	O = intermediate intensity L = 466 P = 226 LPS = 2	30 mm regional enh.	Vision
15	41	BRCA1	IDC + DCIS	III	O = very high L = 518 M = 162 LMS = 3.1	O = very high L = 350 P = 94 LPS = 3.7	20 mm mass-like enh.	Vision
16	56	BRCA1	IDC + DCIS	II,III	O = very high L = 574 M = 146.5 LMS = 3.9	O = very high L = 709 P = 210 LPS = 3.3	5 x 18 mm small contiguous foci rc 3 mo, 10 x 18 mm dendritic extension	Vision

(continued)

(continued) Table 3

Pt no.	Age at exam	Genetic status	Histology	Grade	T2 SI Muscle/parenchyma score LMS	T2 SI Lesion/parenchyma score LPS	Lesion size	MR Device
17	48	BRCA2	IDC + ILC	III	O = low intensity L = 133 M = 89.5 LMS = 1.4	O = low intensity L = 150 P = 150 LPS = 1	8 x 2 mm ductal enh. rc 6 mo, 10 x 4 mm small contiguous foci	Vision
18	59	HFR	Invasive tubular carcinoma	I	ND	ND	10 mm mass-like enh.	Vision
19	44	BRCA1	Invasive carcinomas	ND	O = very high L = 356.5 M = 39 LMS = 9.1	O = very high L = 155 P = 40 LPS = 3.8	6 mm mass-like enh. rc 4 mo, 14 mm mass-like enh.	Avanto
20	42	BRCA1	IDC + DCIS	III	O = intermediate intensity L = 398 P = 254 LPS = 1.5	O = intermediate intensity L = 260 P = 150 LPS = 1.7	6 mm mass-like enh.	Vision
21	43	BRCA1	IDC + LCIS	III	O = intermediate intensity L = 382 M = 117 LMS = 3.2	O = intermediate intensity L = 385 P = 250 LPS = 1.5	13 mm mass-like enh.	Vision
22	42	BRCA2	IDC + DCIS	III	O = very high L = 395.5 M = 58 LMS = 6.8	O = very high L = 420 P = 90 LPS = 4.6	15 mm mass-like enh.	Avanto
23	47	BRCA	IDC	III	O = very high L = 189 M = 37 LMS = 5.1	O = very high L = 185 P = 55 LPS = 3.3	10 mm mass-like enh.	Avanto
24	54	BRCA1	IDC	III	O = very high L = 1152 M = 73.5 LMS = 15.6	O = very high L = 850 P = 200 LPS = 4.2	5 x 18 mm dendritic enh. rc 12 mo, 12 x 18 mm mass-like enh.	Vision
25	50	BRCA2	DCIS + LCIS	II	O = very high L = 514 M = 109 LMS = 4.7	O = very high L = 573 P = 210 LPS = 2.7	12 mm mass-like enh. rc 4 mo, unchanged	Vision
26	40	BRCA1	IDC	III	O = very high L = 998 M = 91 LMS = 10.9	O = very high L = 1000 P = 230 LPS = 4.3	25 mm mass-like enh.	Vision
27	63	BRCA1	IDC	III	O = very high L = 232 M = 37.5 LMS = 6	O = very high L = 350 P = 50 LPS = 7	5 mm mass-like enh.	Avanto
28	61	HFR	IDC + ILC	II	O = very high L = 490 M = 26 LMS = 18.8	O = very high L = 600 P = 200 LPS = 3	18 + 7 + 8 mm mass-like enh.	Vision
29	62	HFR	IDC	II	O = very high L = 465 M = 100 LMS = 4.6	O = very high L = 446 P = 180 LPS = 2.4	20 mm mass-like enh.	Vision
30	52	BRCA2	IDC + DCIS	II	O = very high L = 531 M = 52 LMS = 10	O = very high L = 450 P = 85 LPS = 5.2	8 mm mass-like enh. rc 6 mo, 16 mm mass-like enh + irregular flare	Avanto
31	39	BRCA 1	IDC+DCIS	II	O = very high L = 527 M = 62 LMS = 8.5	O = very high L = 500 P = 60 LPS = 8.3	16 mm mass-like enh., some contiguous rc 4 mo, 30 mm mass-like enh., some more contiguous	Avanto
32	56	BRCA1	LCIS 20 mm + ductal hyperplasia with atypical foci	ND	O = very high L = 218 M = 39.5 LMS = 5.5	O = very high L = 280 P = 50 LPS = 5.6	4 mm mass-like enh.	Avanto
33	39	BRCA1	Adenosis		O = isointensity L = 385 M = 87 LMS = 4.4	O = isointensity L = 394 P = 297 LPS = 1.3	30 mm irregular shape	Vision
34	48	BRCA1	Adenosis		O = very high L = 364 M = 24 LMS = 15.1	O = very high L = 350 P = 40 LPS = 8.7	9 mm mass-like enh.	Avanto

(continued)

(continued) **Table 3**

Pt no.	Age at exam	Genetic status	Histology	Grade	T2 SI Muscle/parenchyma score LMS	T2 SI Lesion/parenchyma score LPS	Lesion size	MR Device
35	37	BRCA1	Dysplasia		O = intermediate intensity L = 355 M = 48 LMS = 7.3	O = intermediate intensity L = 373 P = 246 LPS = 1.5	25 mm irregular shape	Avanto
36	40	HFR	Benign disease nos		No suspicious findings	No suspicious findings		Avanto
37	54	BRCA1	Stromal fibrosis		No suspicious findings	No suspicious findings		Avanto
38	45	BRCA1	Phyllodes tumor		O = very high L = 466 M = 188 LMS = 2.4	O = very high L = 466 P = 252 LPS = 1.8	6 mm mass-like enh.	Avanto

HFR, women at high familial risk; ND, not done; IDC, invasive ductal carcinoma; DCIS, ductal carcinoma *in situ*; ILC, invasive lobular carcinoma; LCIS, lobular carcinoma *in situ*; T2 SI, signal intensity; O, optical impression; L, T2 value of the lesion; P, T2 value of the parenchyma; LMS, lesion/muscle score; LPS, lesion/parenchyma score; nos, not otherwise specified.

Mammographic findings

Twenty-five (25/34, 73.5%) breast cancers occurred in women with normal mammograms. For 1 of these patients, mammography was not available but was reported as negative. Of 12 recalls requested on the basis of MRI findings, 3 mammographies disclosed positive findings (3/12, 25%).

Eight cancers appeared as a mass, none with smooth margins (Table 1). Four cancers were detected because of microcalcifications with/without association to a true mass. None of these cancers appeared as an architectural distortion; 2 of them appeared as an asymmetrical thickening. None of them had a typically benign appearance like a fibroadenoma, and only 1 showed benign calcifications.

The mammographic density patterns in women with invasive or intraductal breast cancer and false-negative findings on mammograms was not significantly different from those in women with true-positive results.

Ultrasound findings

Sixteen (16/34, 47%) breast cancers occurred in women with normal or benign aspects within the parenchyma. For 1 of these patients, ultrasound was not available but was reported as negative. Of 12 recalls requested on the basis of MRI findings, 4 ultrasound examinations disclosed positive findings (4/12, 33%). All of the 16 cancers appeared as a solid mass with an irregular shape and margins (Table 1). None of these cancers appeared as fibroadenoma-like lesions, round or oval in shape, with posterior acoustic enhancement (Table 1).

As regards false-positive results of conventional imaging, for patient 36, mammography gave negative results within a P2 glandular context. Ultrasound showed a

highly suspect ill-defined hypoechoic mass in a high-familial-risk patient, without MRI correspondence. Histology was negative for cancer.

For patient 37 (BRCA1-mutated), mammography showed the onset of suspected microcalcifications within a P2 mammographic pattern. MRI did not disclose suspicious findings. Histology revealed stromal fibrosis. Patient 38 was negative at mammography but in a P2 glandular pattern. Ultrasound detected a hypoechoic mass with circumscribed margins, considered as iconographically benign, but worthy of biopsy because of the clinical context. In this case, MRI showed a round mass-like enhancement of 6 mm in the same position, with a very high T2 SI, but with an aspecific dynamic curve, which induced the MR radiologist to advice simple follow-up. Histology revealed a phyllodes tumor.

MRI findings

Of the 34 diagnosed breast cancers of our cohort, only 33 were evaluated by means of MRI because 1 patient refused the examination. For one of these lesions (patient 11, right breast), we do not have histology, but the suspect enhancing area showed the same morphologic-kinetic aspects as the biopsied disease of the contralateral breast.

None of the 33 MRI-evaluated cancers occurred in a benign or negative context, hence MRI did not register false-negative results. However, we considered as suspect and sent to biopsy 2 cases of adenosis and 1 complex dysplasia.

Of malignant lesions, the most frequent morphologic pattern was enhancing mass-like in 26 patients (26/33, 78%), round or oval shape, single or more than one contiguous foci, each one a few millimeters in size in the second case (Table 2). Of these 26, 11 (11/26, 42%) le-

Table 4 - Histological results

Pt no.	Age (yr)	Gene mutation	Previous breast cancer	Histology	Grade	ER, PgR, p185 (Her2neu)
1	43	BRCA 1		IDC with medullary aspects	III	ER-, PgR-, p185 0
2	60	BRCA 1		IDC	III	ER-, PgR-, p185 2+
3	61	BRCA 1		IDC		ER-, PgR-, p185 3+
4	35	BRCA 2		ILC + LCIS	III	ER-, PgR-, p185 2+
4bis	40			IDC	II	ER+, PgR-, p185 2+
5	58	HFR		IDC	I	ER+, PgR+, p185 ND
6	52	BRCA 1		IDC	III	ER-, PgR-, p185 0
7	48	BRCA 1		IDC with medullary aspects + DCIS	III	ER-, PgR-, p185 3+
8	63	BRCA 1		DCIS	III	ER-, PgR-, p185 2+
9	52	BRCA 1		IDC	II	ER-, PgR-, p185 2+
10	38	BRCA 1		IDC	III	ER-, PgR-, p185 2+
11	61	BRCA 2		left: IDC + DCIS right: no biopsy	III -	ER+, PgR-, p185ND -
12	46	BRCA 1		IDC	III	ER-, PgR-, p185 0
13	56	HFR		IDC pure mucinous subtype + DCIS	III	ER-, PgR-, p185 3+
14	50	HFR	Contralateral (DCIS + LCIS)	DCIS + LCIS + pagetic extension to ducts	II	-
15	41	BRCA 1		IDC + DCIS	III	ER-, PgR-, p185 0
16	56	BRCA 1		IDC + DCIS	II,III	ER-, PgR-, p185 0
17	48	BRCA 2	Contralateral nos	IDC + ILC	III	ER-, PgR-, p185 2+
18	59	HFR		Invasive tubular carcinoma	I	ER-, PgR-, p185 0
19	44	BRCA 1		Invasive carcinoma Not otherwise specified	ND	ER-, PgR-, p185 0
20	42	BRCA 1		IDC + DCIS	III	ER-, PgR-, p185 0
21	43	BRCA 1		IDC + LCIS	III	ER-, PgR-, p185 0
22	42	BRCA 2		IDC + DCIS	III	ER-, PgR-, p185 3+
23	47	BRCA 1		IDC IDC + ILC Benign mastopathy	III II -	ER+, PgR+, p185 1+ - -
24	54	BRCA 1		IDC	III	-
25	50	BRCA 2	Contralateral IDC + ILC	DCIS + LCIS	II	ER-, PgR-, p185 3+
26	40	BRCA 1		IDC	III	ER-, PgR-, p185 2+
27	63	BRCA1		IDC	III	-
28	61	HFR		IDC + ILC	II	ER+, PgR-, p185 1+
29	62	HFR		IDC	II	ER+, PgR-, p185 1+
30	52	BRCA2		IDC + DCIS	II	ER+, PgR-, p185 0
31	37	BRCA 1		IDC + DCIS	II	ER+, PgR-, p185 0
32	56	BRCA 1	Contralateral nos	LCIS 2 m + ductal hyrplasia with atypical foci	ND	-
33	39			Adenosis		
34	48			Adenosis		
35	37			Dysplasia		
36	40	HFR		Benign disease nos		
37	54	BRCA 1		Stromal fibrosis		
38	45	BRCA 1		Phyllodes tumor		

IDC, invasive ductal carcinoma; DCIS, ductal carcinoma *in situ*; HFR, high familial risk; ILC, invasive lobular carcinoma; LCIS, lobular carcinoma *in situ*; ER, estrogen receptor; PgR, progesterone receptor; p185 (Her2neu), expression of the oncoprotein p185 (Her2neu); nos, not otherwise specified.

sions showed smooth margins and homogeneous internal enhancement. One of these converted to an irregular shape made by several contiguous dendritic aspects, irregular borders and hence heterogeneous enhancement (patient 16). It was an IDC combined with a DCIS, in a mutated-BRCA1 patient. Another lesion converted to irregular borders but still with homogeneous uptake at the recall (patient 30). It was also an IDC combined with a DCIS, but in a BRCA2 carrier. For the remaining 9, 4 were pure IDC, 1 was invasive cancer not otherwise specified, 3 were IDC commixed with DCIS, and 1 was DCIS and LCIS. Of these 11 malignancies arising with smooth margins and homogeneous internal enhancement, 9 were in BRCA1 and 2 in BRCA2 carriers.

The T2 SI in these mass-like lesions with smooth margins and homogeneous internal enhancement was high in 9 (9/11, 81%) and of intermediate intensity in 1, whereas the T2 IR sequence resulted not done in 1 (Table 2). When of intermediate intensity, histology revealed IDC and DCIS.

Of the 26 tumors with a morphologic mass-like pattern, 15 (55.5%) demonstrated irregular borders: 9 were pure IDC, 1 was invasive tubular carcinoma, 1 was ILC and LCIS, 1 was IDC and LCIS, 2 were IDC and DCIS, and the last was IDC and ILC. Eight of these breast cancers belonged to BRCA1-mutated women, 4 to BRCA2-mutated women, and 3 to women at high familial risk.

The T2 SI in mass-like lesions with irregular borders was very high in 10 (10/15, 66.6%), of intermediate intensity in 2, low in an IDC, and not done in 2. When of intermediate intensity, histology revealed IDC in one and IDC and LCIS in the other. Of these 15 lesions with irregular borders, 6 were associated to the rim pattern (Table 2).

Seven of 33 MRI-detected cancers did not show a typical mass-like morphologic enhancement (7/33, 21%). Four of them arose as an irregular shape with speculated borders; 2 as dendritic, ductal but very irregular, with speculated edges and a branched aspect; and 1 as a more linear, ductal-like enhancement.

Irregular shapes with irregular margins mainly occurred in *in situ* carcinomas (1 DCIS, 1 not submitted to biopsy but with the same shape as in the contralateral DCIS, and 1 DCIS and LCIS) except for 1 IDC: 2 of the women were at high familial risk and the remaining were BRCA2-mutated. T2 SI was low in those not biopsied, of intermediate intensity in the case of DCIS and LCIS, and very high in one DCIS and one IDC. None of the lesions characterized by a regular shape at presentation showed any morphological transformation at the recall.

Dendritic aspects were present in BRCA1 subjects and histology disclosed DCIS in one case and IDC in the other. T2 was of intermediate intensity in intraductal disease and of high intensity in invasive cancer. Both of the diseases characterized by dendritic morphology at presentation demonstrated a transformation at the recall: the lesions converted into a mass-like enhancement in both subjects. These mass-like entities were always combined with irregular margins, but with homogeneous uptake in one and rim enhancement in the other (Table 2).

Ductal enhancement was associated to a BRCA2-mutated patient with IDC and ILC (Table 2). T2 SI was of low intensity. The lesion converted into several contiguous round small mass-like enhancements at the recall.

As regards false-positive MRI results, morphologic pattern was that of an enhancing mass, with smooth margins and homogeneous enhancement combined with a plateau curve in one case of adenosis, where T2 was very high and the patient was BRCA1 mutated. One case showed an irregular area of enhancement with very irregular margins and heterogeneous enhancement and a steady curve. The T2 SI was isointense compared to normal parenchyma; the patient was BRCA1 mutated. The third case, in a BRCA1-mutated patient, was an irregular area of enhancement, irregular in shape, with homogeneous uptake, with a plateau curve and T2 SI of intermediate intensity.

Concerning dynamic aspects, of 33 MRI-analyzed cancers, 21 were associated with a washout curve shape (21/33, 63.6%). In 1 case the washout curve showed a delayed aspect as may happen in the lobular histotype¹². In another one, the washout curve was commixed with a steady curve at presentation but converted to a washout

type, the only kinetic aspect at the recall (Table 2). A third lesion registered a washout type at presentation but converted into a steady type at the recall.

Seven other neoplasms were associated with a plateau curve shape (7/33, 21%) and 5 (5/33, 15%) to a steady curve shape, one of which converted to a washout shape at the recall (Table 2).

Of the 21 washout curves, 13 (13/21, 61.9%) belonged to pure invasive carcinoma, 5 (5/21, 23.8%) to invasive carcinoma combined with intraductal disease, and 3 (3/21, 14%) to *in situ* disease alone. This curve shape was found in 10 BRCA1-mutated, 6 BRCA2-mutated, and 5 high-familial-risk patients.

Of the 7 plateau type curves, 4 (4/7, 57%) were found in pure invasive carcinoma, 2 (2/7, 28.5%) belonged to invasive carcinoma combined with intraductal disease, 1 corresponded to the lesion not submitted to biopsy, and none was associated to intraductal disease. Of these 7, 5 were found in BRCA1- and 2 in BRCA2-mutated women.

Of the 5 steady curves, 2 (2/5, 40%) were invasive carcinoma, 2 (2/5, 40%) belonged to invasive carcinoma combined with intraductal disease, and 1 (1/5, 20%) was present in intraductal disease. They were found in 4 BRCA1- and 1 BRCA2-mutated women.

Benign disease was never associated with a washout curve and always found in BRCA1-mutated women.

T2 signal intensity

Considering the 33 MRI-detected cancers, T2 IR sequence was not applied in 3 cases. Of the other 30, we accounted for 22 breast cancers with very high T2 SI (22/30, 73%), 5 breast cancers showed T2 SI of intermediate intensity (5/30, 16.6%), and 3 cancers were associated to low T2 SI (3/30, 0.1%) (Table 2). Of the 3 MRI false-positive cases, 1 was isointense on T2 sequence, 1 showed intermediate intensity and 1 showed high T2 SI.

Of the 22 neoplasms with high T2 SI, 13 were found in BRCA1-mutated (13/22, 59%), 7 in BRCA2-mutated (7/22, 31.8%), and 2 in high-familial-risk patients (2/22, 0.1%). Of the 5 lesions with T2 intermediate intensity, 4 were associated to BRCA1 mutation and 1 to high familial risk. For the 3 low intensity T2 SI cancers, 2 were associated to BRCA2 and 1 to BRCA1 mutation.

Of the 22 with high T2 SI, 14 (14/22, 63.6%) were pure invasive carcinoma, 3 (3/22, 13.6%) were pure intraductal disease, and 5 (5/22, 22.7%) were invasive carcinoma associated to intraductal disease. Of the 5 cancers with intermediate T2 SI, 2 were pure *in situ* disease, 1 was pure IDC, and 2 were invasive combined with intraductal disease. Lastly, of the 2 lesions with low T2 SI, 1 was IDC and the other was not submitted to biopsy.

To evaluate the brightness of SI on T2 IR sequences, we quantified T2 SI of the lesion by means of two functions: first the pixel lens value, second an ROI. The former compared the SI of the lesion to the one of the sur-

rounding parenchyma, the latter to the SI of the pectoralis major muscle.

As regards the LPS, in our cohort we found that optical low SI corresponded to a value ≤ 1.2 , whereas intermediate SI ranged from 1.2 to 2.5 and high SI over 2.5 (Table 3). As regards the lesion-to-muscle score (LMS), we also registered some basal thresholds (Table 3). Many overlaps occurred in this case between the numeric results. In detail, optical low SI ratio values between SI of the lesion and the pectoralis major muscle ranged from 1.4 to 2.5. One patient with cancer relapse over a previous surgical scar had a score of 5.9 in low optical SI. Optical middle SI numerical scores ranged from >1.5 to <4 ; and high SI between 3.1 and 18.8 (Table 3).

Several overlaps occurred between numerical scores of middle and high SI. Low SI values were between 1.4 and 2.5, with the exception of one lesion arising over a previous surgical scar that registered an optical low T2 SI but with a corresponding LMS score of 5.9 (patient 10). The highest SI scores were found in patients 24, 26, 28 and 30 (Tables 2 and 3). Corresponding optical brightness was cystic-like for all the lesions, two of which also showed rapid growth. Only one lesion arose over a previous scar. Two of these were pure IDC, grade III; one was IDC and ILC, grade II; the last was DCIS and IDC, grade II.

Patients 8, 11 (right), 15 and 20 exhibited some discrepancies. The tumor of patient 8 showed optically intermediate T2 intensity with an LMS score of 1.5, like lower LMS general scores. However, it was a DCIS. For patient 11, the tumor (on the right) was of low optically T2 intensity but with a 2.5 LMS score, like intermediate LMS scores. We do not know the histology of the lesion. The tumor of patient 15 demonstrated an optically high T2 but the LMS score was of the intermediate group, and the lesion was an IDC and DCIS, grade III. The tumor of patient 20 showed an optically intermediate T2 intensity, but the LMS score was of the lower LMS general scores. Again, the lesion was an IDC and DCIS, grade III.

Imaging phenotype

Of the 31 women affected by breast cancer, 1 refused MRI because of claustrophobia and the disease was detected only with mammography and ultrasound. In 15 patients, the diagnosis of breast disease was made after the first MRI examination was performed (and 5 of these had previously been evaluated only by means of conventional analysis). Sixteen had the onset of disease during the screening program, and the cancer arose after an interval of 3 years for one woman and of 1 to 2 years for the others. Two different expert radiologists reviewed previous MRI of these women and confirmed the absence of morphologic or dynamic indications of a tumor.

For 9 of the group already enrolled in the surveillance program (9/16, 56.3%), MRI examinations preceding

the onset of the disease were completely negative, with bilateral darkness of both breasts on early and late subtracted images. For the remaining 7 (7/16, 43.7%), the former MRI showed a dysplastic pattern, with bilateral multiple foci of enhancement almost of the same size, as is frequently seen in young women.

Owing to the possibility of false-positive results of MRI, when an MRI examination was suspect but without corresponding findings on mammography or ultrasound, the patients were deferred to follow-up. This happened for 12 cases (Table 2). As we had previously noted that some changes may occur in mammary parenchyma of BRCA-mutated women within short periods, we reduced the period of follow-up to a few months. Only one of these patients with suspicious aspects on MRI but with no correspondence on conventional imaging delayed the MRI control to one year because of claustrophobia.

On the last recall (Table 2), only 4 of the 12 (4/12, 33.3%) had no change, whereas we noted a volume increase besides some morphological or dynamic changes of the disease in the other 8 (8/12, 66.6%) cases. Changes occurred for periods ranging from 3 months to 1 year. Of patients who had a phenotypic evolution, 6 were BRCA1 mutated (6/8, 75%), 2 were BRCA2 mutated (2/8, 25%), and none were at high familial risk. Tumors with unchanged morphological and dynamic aspects were from patients at high familial risk in 2 cases, BRCA1 mutated in 1, and BRCA2 mutated in the remaining subject. All changes that occurred in 3 months were in BRCA1-mutation carriers.

Of the 8 tumors that experienced an MRI phenotype evolution (Table 2), 2 had an impressive volumetric increase of nearly 1 cm, respectively at 3 months and 1 year (patients 19 and 24). Both of them were BRCA1-mutation carriers, and the cancer histotype was invasive carcinoma not otherwise specified in the first and IDC in the second. Their age was 44 and 54 years. For the first woman, morphology evolved from a small focus of enhancement, smooth margins and homogeneous uptake of contrast medium to a larger enhancing mass, with a rim pattern and speculated margins, highly suggestive of an infiltrative behavior. The diameters changed from 6 to 14 mm in 3 months (Figure 1). In this case, mammography remained unsuspecting at the recall, whereas ultrasound depicted a structural nonhomogeneity as a focal architectural distortion without typical characteristics for cancer on the basis of MRI findings. Mammographic glandular pattern was P2 according to the Wolfe Classification¹³.

The second woman had a dendritic impregnation (ductal like with speculated-branched margins) at the beginning, with speculated borders and heterogeneous enhancement, and the evolution was towards a single larger mass-like lesion, again with irregular margins and a rim pattern. Hence in this case, besides the volumetric increase, also morphologic phenotype showed a trans-

formation in a short time. The size of the lesion changed from 5 x 18 mm to 12 x 18 mm within 12 months (Figure 2). Mammographic glandular pattern was again P2, and conventional imaging (both mammography and ultrasound) remained unsuspecting at the recall. In contrast, dynamic parameters did not show any transformation between the first MRI examination and the recall.

Considering the high speed of growth, it was expected that the most typical malignant feature in terms of kinetics occurred in the 2 cases. Surprisingly, both diseases were not associated to a washout curve but to a steady-curve type in the first and a plateau type in the second case. Another interesting morphologic pattern was the T2 SI, which was very high in both cases from the beginning.

Also for the tumor of patient 23 (Figure 3), there was a volumetric increase in a mass-like enhancement, ill-defined margins, and homogeneous uptake of 11 x 13 mm in a morphologically unchanged enhancing mass of 13 x 20 mm. Changes occurred within 3 months. In this case, besides the volumetric increase, we noted the onset of two further pathological foci of 7 and 6 mm (Figure 3). The main lesion was not associated with a rim pattern. Also in this case, the patient showed BRCA1 mutation and was 47 years old. The mammographic glandular pattern was P1. Conventional imaging was also positive in this case, but the patient refused surgery for 3 months. Mammography showed a mass with indistinct margins. Ultrasound depicted an ill-defined hypochoic mass. In this subject, kinetic aspects also showed an evolution and once again, surprisingly, the change was from washout to a steady shape of the dynamic curve. T2 SI was again very high. Histology showed IDC for the major lesion. Regarding the smaller lesions, one belonged to an IDC and ILC and the second to a benign mastopathy.

Similar morphologic evolution but with a smaller diameter occurred in patient 8 (Figure 4). In this case, tumor growth was of a few mm, the T2 SI was of intermediate intensity, and histology revealed a pure DCIS. The lesion arose as a tiny dendritic enhancement of 2 x 10 mm, ductal like with speculated borders, and converted to a single mass of 15 mm in 3 months, with speculated margins without a rim pattern. T2 SI was in this case of intermediate intensity. In contrast, dynamic parameters did not show any change like the washout type. Glandular pattern was N1. On occasion of the recall, ultrasound did not reveal any abnormal finding, whereas mammography disclosed the onset of some calcifications within an asymmetric structural thickening, where MRI showed the suspicious enhancement. However, morphology and density of calcifications were not typical of malignancy. The patient was BRCA1 mutated, 63-years old, and histology disclosed DCIS. In this case, chemotherapy could be avoided.

For another patient (patient 17), we registered a smaller increase in the medio-lateral diameter, resulting

from a numerical increase in some contiguous enhanced ducts, suggestive of endoductal proliferation. Diameters converted from 2 x 8 mm to 4 x 10 mm in 6 months. Margins of the region of enhancement were speculated from the beginning. Dynamic parameters did not show any change like the washout type. T2 SI was also very high in this case. The mammographic pattern was N1, but conventional imaging remained unsuspecting at the recall. The patient was BRCA2 mutated, 48-years old, and histology disclosed IDC and ILC.

Patient 16 experienced an onset of the disease represented by several small round foci, smooth borders and homogeneous enhancement along a ductal-like extension. Within only 3 months, the disease showed both a volumetric increase and a morphologic phenotype evolution, converting from 5 x 18 to 10 x 18 mm and becoming a non-mass-like irregular area of enhancement in which several contiguous branches of almost dendritic enhancement were represented (Figure 5). The mammographic glandular pattern was P2. Despite MRI findings, also in this case mammography continued to give negative results at the recall, whereas ultrasound disclosed a nonhomogeneous but non-specific area within the same quadrant. The dynamic parameter remained a washout type, T2 SI was very high, and the patient, 56-years old, was BRCA1 mutated with DCIS and IDC.

Another patient had onset of the disease with some contiguous round foci of enhancement (patient 31), but in this case they were not distributed along a linear orientation but already with a branched pattern. The small foci had irregular borders and the growth resulted in an increase in their number, thus in a larger area of enhancement. The growth occurred within 4 months. The maximum diameter evolved from 16 mm to 30 mm. The curve shape, a washout type, did not change between the beginning and the recall. The T2 SI was very high. Histology disclosed DCIS and IDC (Figure 6). Radiographic pattern for the woman was P2, and conventional imaging remained unsuspecting at the recall. The patient was BRCA1-mutated and 39-years old.

The last woman with morphologic phenotype evolution had a single round mass at the beginning, smooth margins and homogeneous enhancement (patient 30). The evolution was towards a tiny volumetric increase, still homogeneous but with irregular margins, surrounded by an irregular weak flare of enhancement. The diameters changed from 8 to 12 mm in 6 months. In this case, the kinetic patterns also changed from steady to the washout type (Figure 7). The glandular pattern was P2. Mammography and ultrasound both gave negative results at the recall, but ultrasound showed the onset of a highly suspect axillary lymph node. The patient was BRCA2 mutated and 52-years old. Histology revealed the presence of DCIS and IDC.

Among the remaining 4 patients in follow-up because of suspicious MRI findings, in one the tumor remained almost unchanged in volume, morphology and dynam-

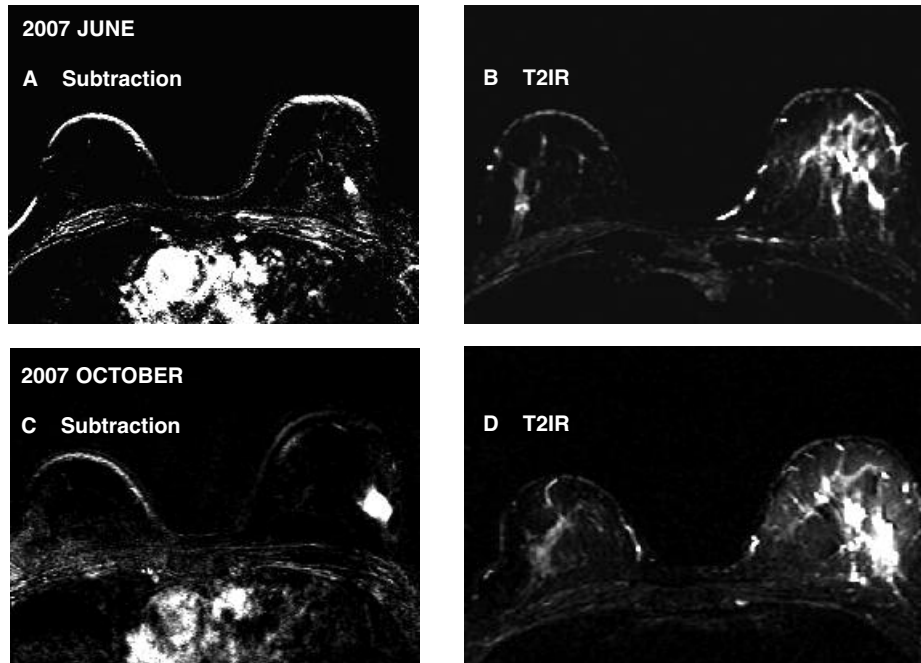


Figure 1 - Patient no. 19. A) Subtraction imaging and B) T2 IR of June 2007. C) Subtraction imaging and D) T2 IR at the recall. Forty-four-year-old patient, BRCA1 mutated, already submitted to breast resection of both mammary parenchyma. A small suspected lesion was seen in the left breast at the first MRI examination (A). Mammography and ultrasound both gave negative results the same day. The mammographic pattern was P2. An impressive volumetric increase in the disease was detected with MRI only 4 months later (C). Note the very high signal intensity of the disease on T2-weighted sequence (B + D). Mammography remained negative. Following the MRI report, ultrasound disclosed the onset of a nonhomogeneous but nonspecific area within the same quadrant. The lesion was an invasive carcinoma, not otherwise classified at histology.

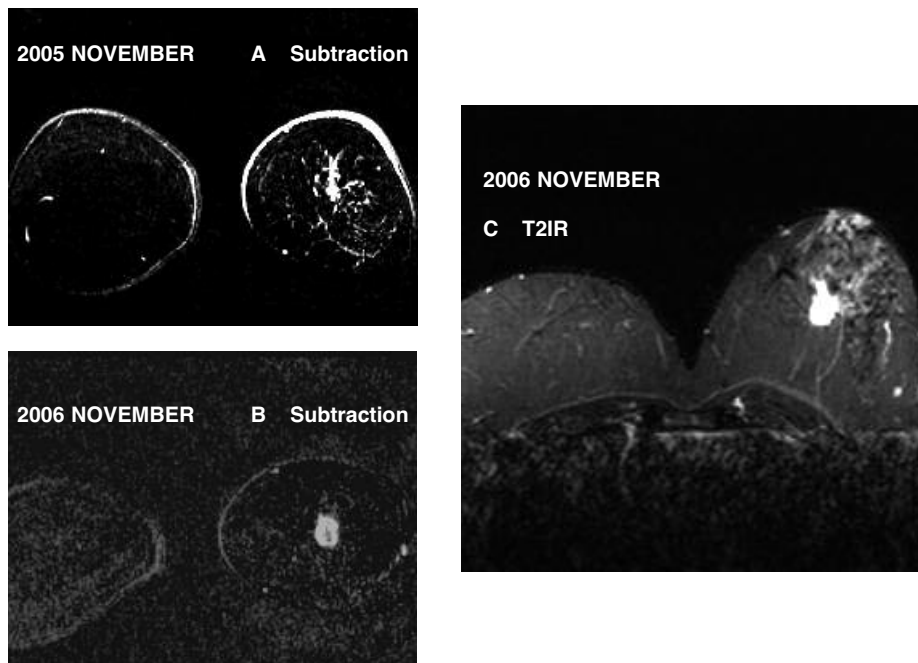


Figure 2 - Patient no. 24. A) Subtraction imaging of November 2005; B) subtraction imaging at the recall; C) T2 IR. Fifty-four years old, BRCA1 mutated, already submitted to breast resection of the right breast. A suspected dendritic enhancement was seen in the left parenchyma at MRI (A). Neither mammography nor ultrasound revealed any abnormal finding. The mammographic pattern was P2. The patient had already been enrolled in our diagnostic surveillance program for one year, and previous MRI was completely negative with uniform darkness of both parenchyma on subtracted images. The patient refused MRI follow-up because of claustrophobia. One year later, previous enhancement was frankly increased, had converted into a mass-like morphologic pattern with irregular margins with rim enhancement (B). Also in this case, the brightness of T2 SI was impressive (C). Mammography and ultrasound were still negative. The lesion corresponded to an invasive ductal carcinoma.

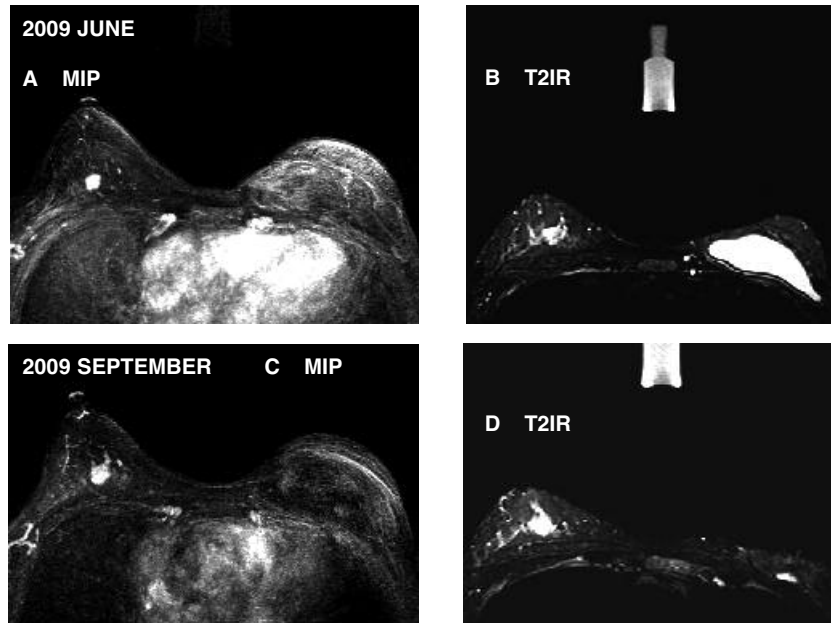


Figure 3 - Patient no. 23. A) Multiplanar intensity projection (MIP) and B) T2 IR of June 2009. C) MIP and D) T2 IR at three recall. Forty-seven year-old patient, BRCA1 mutated, already submitted to left mastectomy for a previous invasive ductal carcinoma. A suspected mass-like enhancement was seen at first MRI (A); high signal intensity and irregular borders (B). Mammography and ultrasound both gave negative results the same day. The mammographic pattern was P1. Only 3 months later, MRI revealed both a significant volumetric increase (C) of the disease and the onset of two more small suspected foci next to the first lesion. The T2 signal intensity of the disease was very high (D). Mammography remained negative. Following the MRI report, ultrasound disclosed the onset of a nonhomogeneous area within the same quadrant. The major lesion was an invasive carcinoma; the smaller foci respectively belonged to a focus of IDC + ILC and to a complex mastopathy. The subject already been part of our diagnostic surveillance program for 7 years, but she had not undergone annual screening (her personal decision). The former MRI was dated 3 years before, when only a dysplastic pattern was detectable. However, even retrospectively, the cancer lesion had arisen in a region where no enhancement was observable on previous examinations.

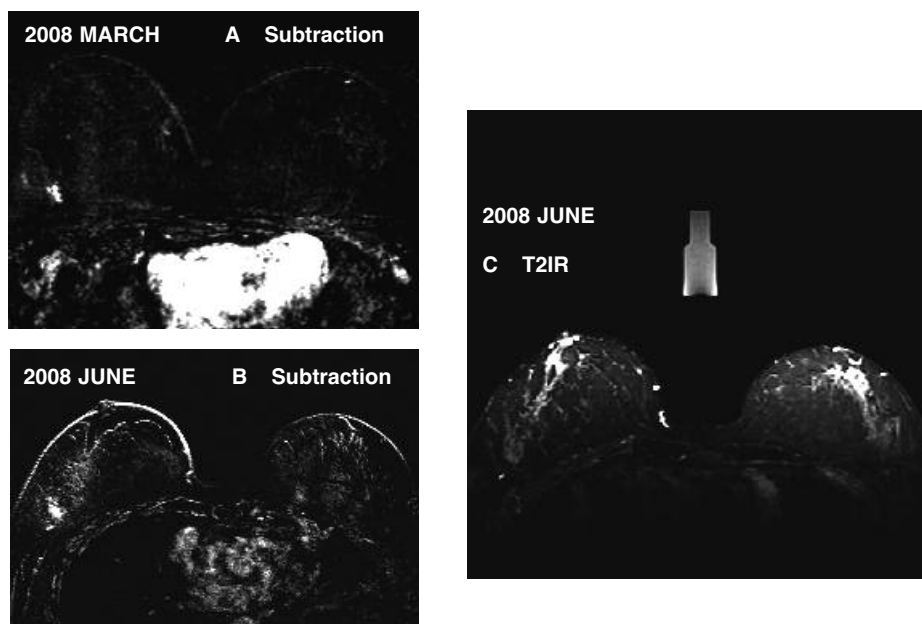


Figure 4 - Patient no. 8. A) Subtraction imaging of March 2008, B) subtraction imaging at the recall, C) T2 IR. Sixty-three year-old patient, BRCA1 mutated. A suspected enhancement was seen in the right parenchyma at MRI (A). Despite an N1 pattern, mammography gave negative results the same day. The patient had been part of our diagnostic surveillance program for 2 years. The former MRI showed a dysplastic pattern with bilateral, small and symmetric multiple foci of enhancement. However, the cancer lesion had arisen in a region where no enhancement was detectable on previous examinations. Only 3 months later, there was an increase in the medio-lateral diameter (B), and mammography showed the onset of calcification in the same quadrant. If evaluated in a general population, the microcalcification would not be judged as suspect because of the morphology and tiny density. The lesion corresponded to a DCIS, and chemotherapy was avoided. In this case, where pure intraductal disease was found, T2 SI was only of intermediate intensity (C).

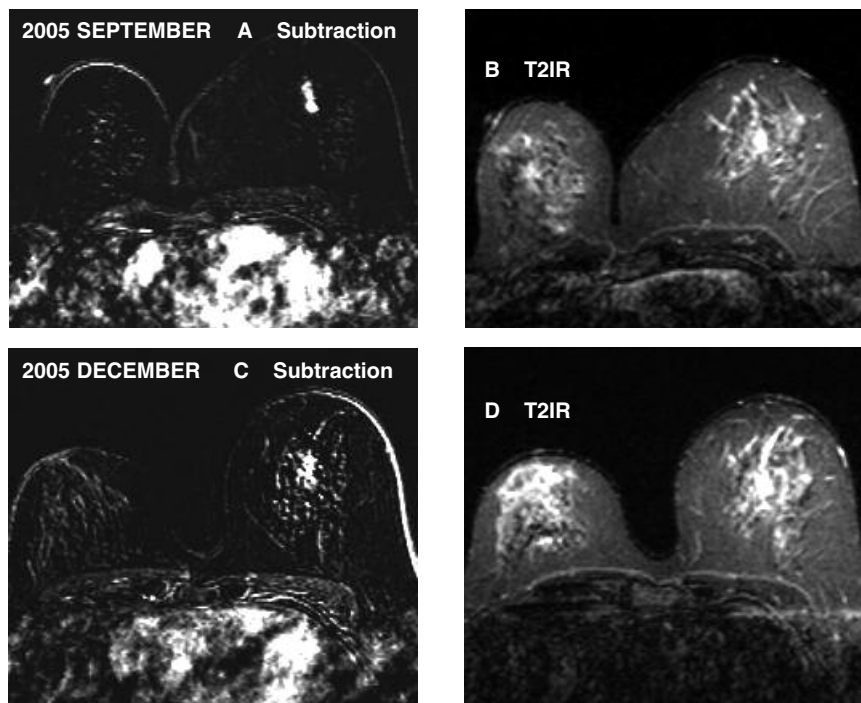


Figure 5 - Patient no. 16. A) Subtraction imaging and B) T2 IR of September 2005. C) Subtraction imaging and D) T2 IR at the recall. Fifty-six years old, BRCA1 mutated, already submitted to breast resection of the right breast. A suspected enhancement was seen in the left parenchyma at MRI (A). Neither mammography nor ultrasound revealed any abnormal finding. The mammographic pattern was P2. The patient had been part of our diagnostic surveillance program for 2 years, and former MRI examinations had not shown any dysplastic pattern of enhancement. After 3 months, there was a volumetric increase in the enhancement and margins turned from smooth to speculated (C). Mammography remained unchanged. Under MRI guidance, ultrasound disclosed a nonhomogeneous area, again not typical of cancer, within the same quadrant. Histology revealed DCIS + IDC. In this case, chemotherapy became necessary. T2 SI was of very high intensity (B + D).

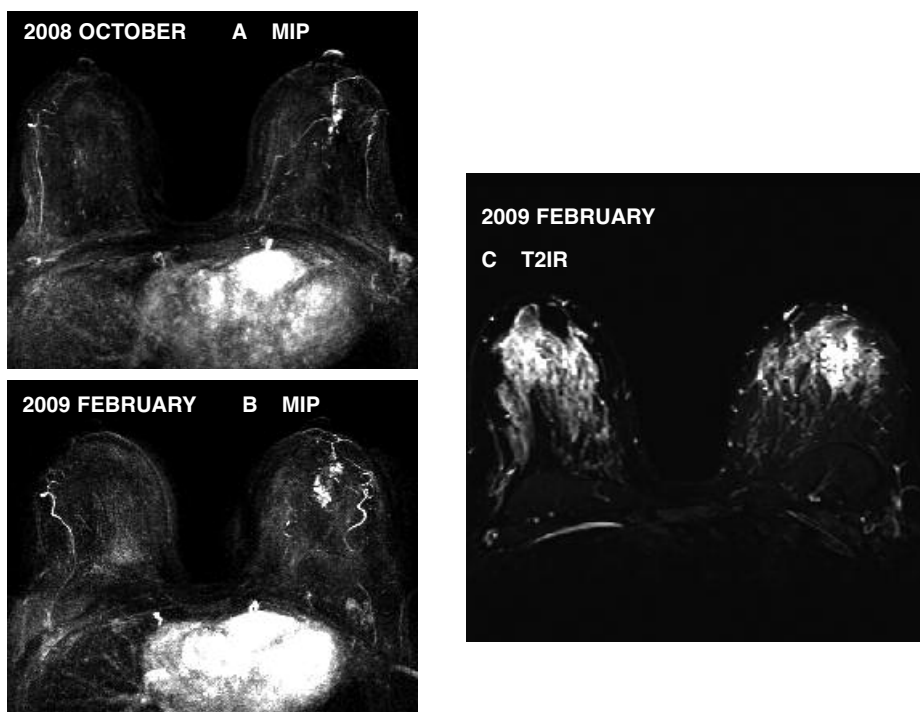


Figure 6 - Patient no. 32. A) MIP of October 2008. B) MIP and C) T2 IR at the recall. Thirty-nine years old, BRCA1 mutated, with P2 mammographic pattern, without any detectable irregularity both mammography or ultrasound. A suspected enhancement was seen in the left parenchyma at the first MRI (A). Only after 4 months, MRI showed a significant enlargement of the pathologic findings (B), whereas mammography and ultrasound were still negative. Histology disclosed DCIS + IDC, and chemotherapy became necessary. T2 SI was still very high (C).

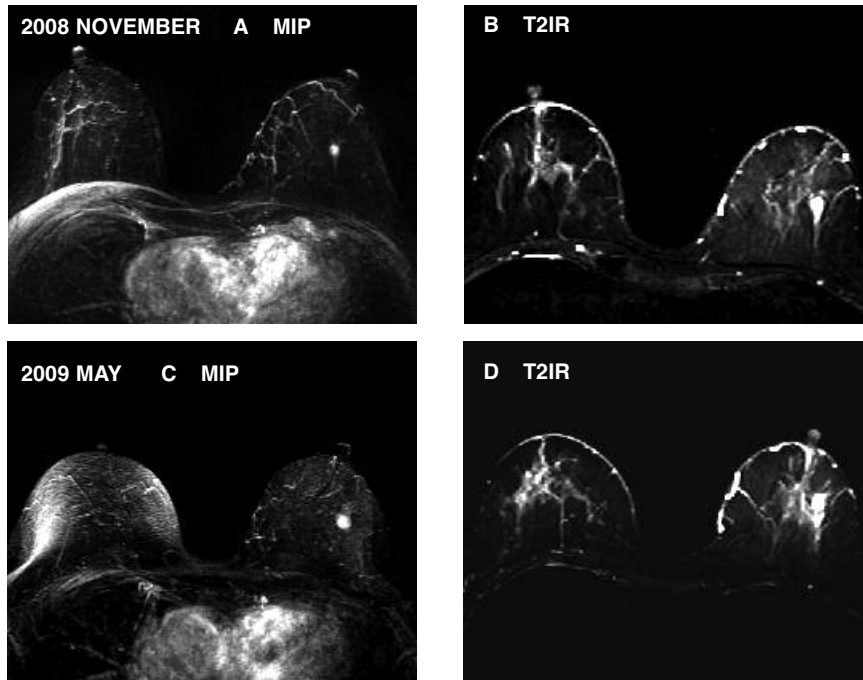


Figure 7 - Patient no.30. A) MIP and B) T2 IR of November 2008. C) MIP and D) T2 IR at the recall. Fifty-two years old, BRCA2 mutated, with P2 mammographic pattern, with no detectable irregularity at mammography or ultrasound. A suspected enhancement was seen in the left parenchyma at MRI (A). The patient had been part of our diagnostic surveillance program for 4 years. Former MRI showed a dysplastic pattern, with bilateral, small and symmetric multiple foci of enhancement. However, the cancer lesion had arisen in a region where no enhancement was detectable on previous examinations. After 6 months, MRI revealed a small enlargement of the pathologic finding, margins turned from smooth into speculated, and a faint enhancement appeared around the lesion (C). We also noted a change in the shape of the dynamic curve: from steady into washout. Mammography and ultrasound still remained negative. Histology disclosed IDC + DCIS. T2 SI was still very high (B + D).

ic aspects for 7 months (patient 14). The lesion was a 6-cm regional enhancement in a 50-year-old woman who had previously been submitted to left mastectomy for multiple foci of DCIS associated with LCIS. The region of enhancement was anterior to an esthetic prosthesis of the remaining breast. The margins of the enhancement were speculated and the curve was a classical washout type mixed with a delayed washout type, which is possible to find in lobular carcinoma¹². Distribution of the enhancement involved homogeneously all the parenchyma, thus raising doubt of just a highly vascularized stroma, but it could not be compared with the contralateral breast because of the mastectomy. Owing to the presence of the prosthesis, evaluation by mammography did not detect any abnormality within the parenchyma, whereas ultrasound disclosed the presence of a single small mass of 1 cm behind the nipple. The mammographic glandular pattern was dysplastic. The patient was a high-risk woman with DCIS and LCIS.

Another patient remained almost unchanged in 4 months, with a volumetric increase of only a few millimeters (patient 29). The morphologic pattern was of an irregular area of homogeneous enhancement and speculated margins. In this case, it was the dynamic curve shape that showed partial evolution. In fact, at the

beginning the ROI on the enhancing region showed steady type mixed with a washout curve, whereas at the recall the curve was only a washout type. Here mammography was not suspicious, whereas ultrasound revealed a poorly defined hypoechoic mass dubious for cancer at the first examination. This area corresponded to an MRI region of enhancement. The same region became more suspect at the recall. The glandular pattern was dysplastic. The patient belonged to the high-familial-risk group, and histology revealed the presence of IDC.

For 2 patients (patients 6 and 25) submitted to recall, an intraductal development of enhancement was detected at the beginning with some contiguous small foci, with speculated margins for the first case and smooth margins for the second. The morphological aspects, the size and the dynamic curve shape (washout type) remained the same at the diagnosis and at the recall, respectively after 5 and 4 months. Despite an N1 pattern for the first case, no suspicious findings appeared at the first analysis, whereas a mass with indistinct margins appeared at mammography. Only at the recall did ultrasound reveal a small, suspicious mass. With an N1 glandular pattern for the second case, ultrasound continued to give negative results, whereas for

the recall some malignant calcifications appeared at mammography. These women were BRCA1 and BRCA2 mutated with respectively IDC and DCIS and LCIS.

All cancers with a more rapid speed of growth (patients 16, 19, 24 and 31) were from BRCA1 mutation carriers (Table 2).

Location of cancer

Schrading and Kuhl¹⁴ described how the location of a breast cancer may become an important predictor of malignancy. They discovered that women with BRCA1 mutation or high familial risk tend to develop breast cancer in the posterior part of the breast.

In our group of 33 MRI-detected breast cancers, 13 lesions were located in the posterior portion of the breast, 11 of them in the prepectoral region. Of these 13 tumors, 7 were from BRCA1-mutated and 4 from BRCA2-mutated patients, and 2 were high-familial-risk patients.

Discussion

There is emerging evidence that tumors in BRCA carriers, compared to sporadic cancers, exhibit different biological and morphological features. BRCA1 breast cancers are frequently poorly differentiated, with higher mitotic counts, negative for estrogen and progesterone receptors, p185 negative and p53 positive. Tumors from BRCA2-mutated women as well as those arising in high-familial-risk women show pathologic features similar to those of sporadic cases¹⁵⁻¹⁷.

Tilanus-Linthorst *et al.*^{15,17} also reported the same tumor behavior we observed in the present study. In fact, they described faster tumor growth in women with BRCA mutation than in the general population and estimated a tumor doubling time of 45 days for mutation carriers. Furthermore, they reported major tumor growth in women with BRCA1 mutation and in patients aged <40 years of age.

In accord with these findings, in our study we noted that an impressive volumetric increase occurred in a short time. Tumors that showed the most rapid growth were in 4 BRCA1 carriers (patients 16, 19, 24 and 31), whereas the age of these patients was 56, 44, 54 and 37 years, respectively. Considering the longest diameter of each enhancing lesion, the increase in size was estimable respectively as 8 mm in 3 months, 8 mm in 4 months, 7 mm in 12 months, and 17 mm in 4 months. Histology was indicative of invasive carcinoma in all 4 cases; except for one case, the tumors were all grade III. Evaluation of hormone receptor was not available in one case, while 2 cases were triple negative and the last one showed Er+PgR-p1850 parameters.

However, it has been observed that radiological phenotype may be different in hereditary breast cancer. In fact, such tumors frequently show morphological and

kinetic aspects commonly seen in benign lesions^{5,14,18,19}. Schrading and Kuhl¹⁴ pointed out a major number of differences in BRCA1-associated cancers. In fact, they did not find calcifications associated with invasive cancer or intraductal disease.

Concerning our cohort, we found 3 intraductal carcinomas (patients 8, 14 and 25), but only one of them, whose histology described DCIS and LCIS, was associated to suspected calcifications (patient 25). For the only pure ductal *in situ* carcinoma (patient 8), tiny, aspecific calcifications were observed, whereas in the remaining case of DCIS and LCIS calcifications were not detectable at mammography because of the presence of a breast prosthesis (Table 1). The first case was a BRCA1 carrier, the second a high-familial-risk woman, and the third a BRCA2 carrier.

Within our group, we detected only 3 cases of pathological calcifications, and these were related to invasive carcinomas (patients 3, 7 and 13) (Table 1). Two of these patients were BRCA1 mutated and the third was at high familial risk.

Tilanus-Linthorst *et al.*⁵ and Kuhl *et al.*¹⁸ also described how BRCA1-associated cancers may exhibit “pushing”, well-circumscribed margins, homogeneous internal architecture, and low echogenicity.

In our patients (Table 1), we noted that when no suspicious findings were detected at mammography mainly because of a glandular pattern, ultrasound could more easily depict pathologic aspects with a higher sensitivity before and after MRI. However, when detectable by means of conventional imaging, breast cancers of our group did not significantly differ from sporadic cancers. In fact, the percentage of hereditary breast cancers with typically benign aspects was very low in our study. As regards MRI, Schrading and Kuhl¹⁴ reported a high percentage of invasive cancers with a non-mass enhancement and a benign kinetic aspect.

Morphologic patterns are usually of eminent relevance in the radiological interpretation. Smooth borders have often been associated with a negative predictive value for malignancy^{9,20}, whereas irregular contour, nonhomogeneous enhancement and rim pattern have been reported as highly indicative of malignancy¹⁵. Tilanus-Linthorst *et al.*¹⁵ stated that the association of rim enhancement with central necrosis can be an indicator for the growth rate of tumors. Jimenez *et al.*²¹ reported that centrally necrotizing carcinomas had an accelerated clinical course and early systemic metastasis. This is in agreement with Tilanus-Linthorst *et al.*¹⁵, who also found mitotic count to be significantly high in tumors from gene-mutation carriers. Regarding our cohort, only 9 of 33 (27%) malignancies showed pure smooth margins: 12 (36%) arose with speculated borders, and 3 neoplasm – initially with smooth margins – converted to irregular margins at the recall.

The higher rate of sharp tumor margins and eventual rim enhancement may thus be explained by the more aggressive nature of tumors in BRCA-mutated carriers.

As regards the correlation with curve shape, the washout type was detected in 21 of the 33 malignancies of our study (21/33, 63.6%). As regards histology, the washout curve was prevalent in invasive carcinoma, but we also found the same curve in intraductal disease. The same curve shape was more often detected in BRCA1-mutated subjects than in the other subjects, but the high number of BRCA1-mutated subjects in our cohort needs to be taken into account. Hence, we can consider the washout curve as highly predictive of malignancy, but without a significant difference between sporadic and hereditary cancers.

For false-positive MRI findings, all the patients were BRCA1 mutated and the morphologic shapes were very suspicious. We did not find the typical washout curve but saw other invasive lesions with the same kinetic aspects. Isointensity of T2 SI should have more favorably directed the diagnosis in one case of adenosis.

Mammography frequently gave false-negative results despite breast density and tumor diameters. One possible explanation could be the major aggressiveness of hereditary cancers, which may reduce the incidence of microcalcifications as an indicator of subclinical, still intraductal lesions.

Moreover, Tilanus-Linthorst *et al.*⁵ described for the first time the phenomenon of prominent pushing margins of breast cancer in BRCA carriers. They observed that when pushing margins are prominent, the fibrotic reaction of the connective tissue adjacent to the tumor and responsible for distortion and spiculated margins is absent. This phenomenon could explain possible false-negative mammograms.

In our experience, the main MRI semeiotic variance that we observed in the group of neoplasms arising in mutation carriers was the T2 SI, which could differ significantly from that of sporadic breast cancers. In fact, it is known that in the general population, T2 SI is of an intermediate intensity for breast cancer, of a higher intensity for benign lesions^{5,22,23}, and of an even greater intensity for cystic entities. The almost constant pattern of an MRI semeiotic aspect that we encountered in positive women of our surveillance program was the high or even very high SI of hereditary cancers (Table 3). Kuhl *et al.*⁴ reported that such behavior may occur in mutated cancers.

In another study, carried out on the general population, Kuhl *et al.*²³ observed that breast cancers displayed a low SI on T2-weighted turbo spin echo (TSE) images in 88/101 cases (87%), whereas 13/101 (13%) cases had an increased SI. They also concluded that the T2 TSE pulse sequence without fat suppression was the only one suitable for lesion characterization, whereas they did not obtain the same significant results on corresponding T2-weighted SPIR (spectral presaturation inversion recovery) TSE images (with fat suppression).

More recently, Ballesio *et al.*²² calculated the ratio between the SI of the nodule and the pectoralis major muscle with an ROI analysis on T2-weighted IR se-

quences. Within the general population, they described a lower T2 SI belonging to malignancies, with 82.4% sensitivity, 77.4% specificity, 80% positive predictive value and negative predictive value.

In our experience, carried out on a population at high risk of inherited breast cancer and on mutated women, we found 34 malignant lesions, 33 were submitted to MRI analysis, only 30 of which were also evaluated with T2 IR sequences. Of these 30 T2 IR evaluated cancers, we found that 22 (22/30, 73.3%) displayed an unmistakable hyperintensity: 59% of these T2 very high SI was associated to BRCA1 mutation, whereas only 39% of them was <50 years old. Also that patient with LCIS in BRCA1 mutation showed very high T2SI. MRI false-positive cases showed T2 isointensity and hyperintensity in 2 cases of adenosis and intermediate intensity in one case of dysplasia.

Of the 22 neoplasms with high T2 SI, only 59% were pure invasive carcinomas. The pattern was also found in 3 pure *in situ* carcinomas, 31% were invasive combined with intraductal disease, and the overall medullary aspects were found only in 3 cases. Therefore, it seems that high T2 IR SI cannot be considered as a specific index of a selective histotype, nor an indicator of a medullary or mucinous component only.

If we refer to the phenomenon of "prominent pushing margins", arising from the analysis of BRCA1/2-related cancers⁵ and described by Lakhani *et al.*^{24,25} as a front of tumor cells not separated by connective tissue, we can make some interesting considerations. According to MRI semeiotic parameters, connective tissue shows low to intermediate T2 SI both on T2 TSE and T2 IR sequences because of the scarcity of water. Considering hereditary breast cancers, the T2 SI should thus become higher and increase to major levels if connective structure and desmoplastic reaction are lacking.

In our study, the tumors with a fast growth (patients 16, 19, 24 and 31) consistently demonstrated a very high T2 SI, which was similar to that of cystic matrix. It seems that the absence of connective architecture within the tumor and the absence of the desmoplastic reaction surrounding the lesions reduces the possibility to restrict cancer growth, thus allowing a major aggressiveness. In addition, we found high T2 SI mainly in invasive carcinomas of mutation carriers, but this aspect was also the most frequent in intraductal disease. Consequently, in our cohort, high T2 SI cannot be considered as a pattern specific of invasive cancer. However, all of the cancers with high T2 SI and rapid evolution occurred in BRCA1 carriers (patients 16, 19, 24 and 31). It would thus be interesting to know whether hereditary breast cancer has a peculiar structure, combined with a different induction to the desmoplastic reaction of the surrounding parenchyma, that could explain these new radiological patterns.

In addition to optical impression, to quantify T2 SI we also calculated the mean SI value of each lesion and re-

lated the SI of the lesion to that of the parenchyma (LPS, parenchyma SI) and to that of the pectoralis major muscle (LMS, muscular SI) by means of two different functions: the pixel lens value for the former and an ROI for the latter (Table 3). As regards LPS, parenchymal SI was different in each patient (range, 30-960), but the results of numerical scores proved to be coherent with optical level of brightness (Table 3). For one tumor (patient 24), optical T2 SI was very high, similar to that of cystic lesions, but the ratio score was at an intermediate level (i.e., 2.4). The lesion had an impressive volumetric growth, containing a necrotic center. The numerical score should therefore be considered as an additional index of its internal nonhomogeneity.

As regards LMS (Table 3), muscular SI was less heterogeneous than parenchymal SI. We noted that they remained at lower levels when the examinations had been performed with a Vision device and on higher levels when performed with Avanto. There were several overlaps between numerical scores of intermediate and high SI for LMS. It may be that the quantification of a mean SI value by means of a ROI is more sensitive to the heterogeneity of the internal structure of a lesion than the computation of the mean SI value by means of several pixel lens values taken from different sites of the same lesion. This is even more evident for larger diameters.

However, LPS and LMS analyses both had the limitation of the small number of subjects examined. Further evaluations are needed to improve the new interpretation models. We therefore deduce that the SI calculated on T2 images (LPS and LMS) should be considered as an adjunct parameter for differential diagnosis of doubtful lesions, but in clinical practice they should not be considered alone. LPS and LMS should be used to confirm a diagnosis ruled out on the basis of established breast MRI criteria, such as dynamic enhancement and morphological data.

Conclusions

BRCA carriers face a high lifetime risk of developing breast cancer. However, evidence indicating whether overall prognosis is worse for women with BRCA-related cancer has not been conclusive. Several studies have shown that annual screening in BRCA-mutated or high-risk women can be significantly helpful to detect breast cancer early^{4,7-10,26,27}. It has also been demonstrated that in multimodality surveillance programs the accuracy of MRI is higher than that of conventional imaging and that combination of the two techniques is needed to avoid unnecessary biopsies^{4,28-33}.

Tumor size and nodal status represent the most important prognostic factors in breast cancer^{31,32}. The survival rates of women with breast cancers <1 cm in diameter and with negative lymph nodes are high, and mortality risk may be appreciably reduced by early tu-

mor detection. However, data on the real impact of an early diagnosis are essential, considering that a high proportion of BRCA1-mutated tumors displays negative prognostic factors such as triple-negative status, and lack of a correlation between tumor stage and metastatic spread has been reported in these patients³³. Although caution is needed, early detection should be offered to women with a gene mutation or with an increased familial risk of breast cancer.

Considering recent studies^{5,15,17} showing the faster speed of growth of cancer in carrier women, we believe that when a suspicious lesion is seen only on MRI, it is legitimate to repeat the examination after 2 or 3 months to avoid false-positive results but at the same time to prevent the rapid spread of the disease. After this period, if the lesion persists, it is correct to proceed with MR-guided biopsy even when conventional imaging remains unsuspecting.

The aim of secondary prevention is detection of cancer at its earliest stage to improve prognosis and to provide some advantage in terms of quality of life, considering that chemotherapy may be avoided in patients with intraductal disease. Mainly for these reasons, it is still debated whether MRI should be proposed twice a year in BRCA1-mutated women.

References

- Hartman LC, Sellers TA, Schaid DJ: Efficacy of bilateral prophylactic mastectomy in BRCA1 and BRCA2 gene mutation carriers. *J Natl Cancer Inst*, 93: 1633-1637, 2001.
- King M, Wieand S, Hale K, Lee M, Walsh T, Owens K, Tait J, Ford L, Dunn B, Costantino J, Wickerham L, Wolmark N, Fisher B: National Surgical adjuvant breast and bowel project: Tamoxifen and breast cancer incidence among women with inherited mutations in BRCA1 and BRCA2; National Surgical Adjuvant Breast and Bowel Project (NSABP-P1): Breast Cancer Prevention Trial. *JAMA*, 286: 2251-2256, 2001.
- Brekelmans C, Seynaeve C, Bartels C, Tilanus Linthorst M, Meiers-Heijboer E, Crepin C, vanGeel A, Menke M, Verhoog L, vd Ouweland A, Obdeijn A, Klijn J: Effectiveness of breast cancer surveillance in BRCA1/2 gene mutation carriers and women with high familial risk. *J Clin Oncol*, 19: 924-930, 2001.
- Kuhl C, Schmutzler R, Leutner C, Kempe A, Wardelmann E, Hocke A, Maringa M, Peifer U, Krebs D, Schild H: Breast MRI screening in 192 high-risk women (proven or suspected carriers of a breast cancer susceptibility gene): preliminary results. *Radiology*, 215: 267-279, 2000.
- Tilanus-Linthorst M, Verhoog L, Obdeijn I, Bartels K, Menke-Pluymers M, Eggermont A, Klijn J, Meijers-Heijboer H, Van der Kwast T, Brekelmans C: A BRCA1/2 mutation, high breast density and prominent pushing margins of a tumor independently contribute to a frequent false-negative mammography. *Int J Cancer*, 102: 91-95, 2002.
- Sardanelli F, Podo F: Breast MR imaging in women at high risk of breast cancer. Is something changing in early breast cancer detection? *Eur Radiol*, 17: 873-887, 2007.
- Leach M, Boggis C, Dixon A, Easton D, Eeles R, Evans D: Screening with magnetic resonance imaging and mammography of a UK population at high familial risk of breast

- cancer: a prospective multicentre cohort study (MARIBS). *Lancet*, 365: 1769-1778, 2005.
8. Kriege M, Brekelmans C, Boetes C, Besnard P, Zonderland H, Obdeijn I, Manoliu R, Kok T, Peterse H, Tilanus-Linthorst M, Muller S, Meijer S, Oosterwijk J, Beex L, Tollenaar R, deKoning H, Rutgers E, Klijn J: Efficacy of MRI and mammography for breast-cancer screening in women with a familial or genetic predisposition. *N Engl J Med*, 351: 427-437, 2004.
 9. Sardanelli F, Podo F, D'Agnolo G, Verdecchia A, Santaquilani M, Musumeci R, Trecate G, Manoukian S, Morasut S, deGiacomi C, Federico M, Cortesi L, Concione S, Cirillo S, Marra V: Multicenter comparative multimodality surveillance of women at genetic-familial high risk for breast cancer (HIBCRI Study): Interim Results. *Radiology*, 242: 698-715, 2007.
 10. Trecate G, Vergnaghi D, Manoukian S, Bergonzi S, Scaperrotta G, Marchesini M, Ferranti C, Peissel B, Spatti G, Bohm S, Conti A, Costa C, Sporeni M, Podo F, Musumeci R: MRI in the early detection of breast cancer in women with high genetic risk. *Tumori*, 92: 517-523 2006.
 11. Kuhl C, Mielcarek P, Klaschik S, Leutner C, Wardelmann E, Gieseke J, Schild H: Dynamic breast MR imaging: are signal time course data useful for differential diagnosis of enhancing lesions in dynamic breast MR imaging? *Radiology*, 211: 101-110, 1999.
 12. Trecate G, Tess JD, Vergnaghi D, Bergonzi S, Mariani G, Ferraris C, Musumeci R: Lobular breast cancer: how useful is breast magnetic resonance imaging? *Tumori*, 87: 232-238, 2001.
 13. Sickles EA: Wolfe mammographic parenchymal patterns and breast cancer risk. *AJR*, 188: 301-303, 2007.
 14. Schrading S, Kuhl C: Mammographic, US, and MR imaging phenotypes of familial breast cancer. *Radiology*, 246: 58-70, 2008.
 15. Tilanus-Linthorst M, Obdeijn I, Hop W, Causer P, Leach M, Warner E, Pointon L, Hill K, Klijn J, Warren R, Gilbert F: BRCA1 mutation and young age predict fast breast cancer growth in the Dutch, United Kingdom, and Canadian Magnetic Resonance Imaging Screening Trials. *Clin Cancer Res*, 13: 7357-7362, 2007.
 16. Palacios J, Honrado E, Osorio A, Cazorla A, Sarrio D, Barroso A, Rodriguez S, Cigudosa JC, Diez O, Alonso C, Lerma E, Sanchez L, Rivas C, Benitez J: Immunohistochemical characteristics defined by tissue microarray of hereditary breast cancer not attributable to BRCA1 or BRCA2 mutations: differences from breast carcinomas arising in BRCA1 and BRCA2 mutation carriers. *Clin Cancer Res*, 9 (10 Pt 1): 3606-3614, 2003.
 17. Tilanus-Linthorst M, Kriege M, Boetes C, Hop W, Obdeijn I, Oosterwijk J, Peterse H, Zonderland H, Meijer S, Eggermont A, deKoning H, Klijn J, Brekelmans C: Hereditary breast cancer growth rates and its impact on screening policy. *Eur J Cancer*, 41: 1610-1617, 2005.
 18. Kuhl C, Kuhn W, Schild H: Management of women at high risk for breast cancer: new imaging beyond mammography. *Breast*, 149: 480-486, 2005.
 19. Veltman J, Mann R, Kok T, Obdeijn I, Hoogerbrugge N, Blickman J, Boetes C: Breast tumor characteristics of BRCA1 and BRCA2 gene mutation carriers on MRI. *Eur Radiol*, 18: 931-938, 2008.
 20. Holland R, Hendriks J, Mravunac M: Mammographically occult breast cancer. *Cancer*, 52: 1810-1819, 1983.
 21. Jimenez RE, Wallis T, Visscher DW: Centrally necrotizing carcinomas of the breast: a distinct histologic subtype with aggressive clinical behaviour. *Am J Surg Pathol* 25: 331-337, 2001.
 22. Ballesio L, Savelli S, Angeletti M, Porfiri M, D'Ambrosio I, Maggi C, DiCastro E, Bennati P, Fanelli G, Vestri A, Mangano L: Breast MRI: are T2IR sequences useful in the evaluation of breast lesions? *Eur J Radiol*, 71: 96-101, 2009.
 23. Kuhl C, Klaschik S, Mielcarek P, Gieseke J, Wardelmann E, Schild H: Do T2 weighted pulse sequences help with the differential diagnosis of enhancing lesions in dynamic breast MRI? *J Magnetic Res Imaging*, 9: 187-196, 1999.
 24. Lakhani S, Jacquemier J, Sloane J, Gusterson B, Anderson T, van de Vijver M, Farid L, Venter D, Antoniou A, Storer-Isser A, Smyth E, Steel C, Haites N, Scott R, Goldgar D, Neuhausen S, Daly P, Ormiston W, McManus R, Scherneck S, Ponder B, Ford D, Peto J, Stoppa-Lyonnet D, Easton D: Multifactorial analysis of differences between sporadic breast cancers and cancers involving BRCA1 and BRCA2 mutations. *J Natl Cancer Inst*, 90: 1138-1145, 1998.
 25. Breast Cancer Linkage Consortium. Pathology of familial breast cancer: differences between cancers in carriers of BRCA1 or BRCA2 mutations and sporadic cases. *Lancet*, 349: 1488-1505, 1997.
 26. Warner E, Plewes DB, Hill KA, Causer PA, Zubovits JT, Jong RA, Cutrara MR, DeBoer G, Yaffe MJ, Messner SJ, Meschino WS, Piron CA, Narod SA: Surveillance of BRCA1 and BRCA2 mutation carriers with magnetic resonance imaging, ultrasound, mammography, and clinical breast examination. *JAMA*, 292: 1317-1325, 2004.
 27. Hagen AI, Kvistad KA, Maehle L, Holmen MM, Aase H, Styr B, Vabo A, Aplod J, Skaane P, Moller P: Sensitivity of breast MRI versus conventional imaging in the diagnosis of BRCA-associated breast cancer in a national prospective series. *Breast*, 16: 367-374, 2007.
 28. Warner E, Plewes DB, Shumak RS, Catzavelos GC, Di Prospero LS, Yaffe MJ, Goel V, Ramsay E, Chart PL, Cole DE, Taylor GA, Cutrara M, Samuels TH, Murphy JM, Narod SA: Comparison of breast magnetic resonance imaging, mammography, ultrasound for surveillance of women at high risk for hereditary breast cancer. *J Clin Oncol*, 19: 3524-3531, 2001.
 29. Kuhl C, Schrading S, Leutner C, Morakkabati-Spitz N, Wardelmann E, Fimmers R, Kuhn W, Schild HH: Mammography, breast ultrasound, and magnetic resonance imaging for surveillance of women at high genetic risk for breast cancer. *J Clin Oncol*, 23: 8469-8476, 2005.
 30. Morris E, Liberman L, Ballon D, Robson M, Abramson AF, Heerdt A, Dershaw DD: MRI of occult breast carcinoma in a high-risk population. *AJR*, 181: 619-626, 2003.
 31. Tilanus-Linthorst M, Alves C, Seynaeve C, Menke-Pluymers MBE, Eggermont AMM, Brekelmans CTM: Contralateral recurrence and prognostic factors in familial non-BRCA1/2-associated breast cancer. *Br J Surg*, 93: 961-968, 2006.
 32. Sant M, Allemani R, Capocaccia R, Hakulinen T, Aareleid T, Coebergh JW, Coleman MP, Grosclaude P, Martinez C, Bell J, Youngson J, Berrino F: Stage at diagnosis is a key explanation of differences in breast cancer survival across Europe. *Int J Cancer*, 106: 416-422, 2003.
 33. Moller P, Evans DG, Reis MM, Gregory H, Anderson E, Maehle L, Lalloo F, Howell A, Aplod J, Clark N, Lucassen A, Steel CM: Surveillance for familial breast cancer: differences in outcome to BRCA mutation status. *Int J Cancer*, 121: 1017-1020, 2007.